

---

**This is an electronic reprint of the original article.  
This reprint *may differ* from the original in pagination and typographic detail.**

**Author(s):** Taylor, M. J.; Cullen, D. M.; Procter, M. G.; Smith, A. J.; McFarlane, A.; Twist, V.; Alharshan, G. A.; Ferreira, L. S.; Maglione, E.; Auranen, Kalle; Grahn, Tuomas; Greenlees, Paul; Hauschild, Karl; Herzan, Andrej; Jakobsson, Ulrika; Julin, Rauno; Juutinen, Sakari; Ketelhut, Steffen; Konki, Joonas; Leino, Matti; Lopez-Martens, Araceli; Pakarinen, Janne; Partanen, Jari; Peura, Pauli; Rahkila, Panu; Rinta-Antila, Sami; Ruotsalainen, Panu; Saadati, Mikael; Sarán, Jan; Schelen, Catherine; Sorri, Oblately deformed isomeric proton-emitting state in  $^{151}\text{Lu}$

**Title:**

**Year:** 2015

**Version:**

**Please cite the original version:**

Taylor, M. J., Cullen, D. M., Procter, M. G., Smith, A. J., McFarlane, A., Twist, V., Alharshan, G. A., Ferreira, L. S., Maglione, E., Auranen, K., Grahn, T., Greenlees, P., Hauschild, K., Herzan, A., Jakobsson, U., Julin, R., Juutinen, S., Ketelhut, S., Konki, J., . . . Doncel, M. (2015). Oblately deformed isomeric proton-emitting state in  $^{151}\text{Lu}$ . *Physical Review C*, 91(4), Article 044322.  
<https://doi.org/10.1103/PhysRevC.91.044322>

All material supplied via JYX is protected by copyright and other intellectual property rights, and duplication or sale of all or part of any of the repository collections is not permitted, except that material may be duplicated by you for your research use or educational purposes in electronic or print form. You must obtain permission for any other use. Electronic or print copies may not be offered, whether for sale or otherwise to anyone who is not an authorised user.

## Oblately deformed isomeric proton-emitting state in $^{151}\text{Lu}$

M. J. Taylor,<sup>1</sup> D. M. Cullen,<sup>1</sup> M. G. Procter,<sup>1</sup> A. J. Smith,<sup>1</sup> A. McFarlane,<sup>1</sup> V. Twist,<sup>1</sup> G. A. Alharshan,<sup>1</sup> L. S. Ferreira,<sup>2</sup> E. Maglione,<sup>3</sup> K. Auranen,<sup>4</sup> T. Grahn,<sup>4</sup> P. T. Greenlees,<sup>4</sup> K. Hauschild,<sup>4,5</sup> A. Herzan,<sup>4</sup> U. Jakobsson,<sup>4,\*</sup> R. Julin,<sup>4</sup> S. Juutinen,<sup>4</sup> S. Ketelhut,<sup>4</sup> J. Konki,<sup>4</sup> M. Leino,<sup>4</sup> A. Lopez-Martens,<sup>4,5</sup> J. Pakarinen,<sup>4</sup> J. Partanen,<sup>4</sup> P. Peura,<sup>4</sup> P. Rahkila,<sup>4</sup> S. Rinta-Antila,<sup>4</sup> P. Ruotsalainen,<sup>4</sup> M. Sandzelius,<sup>4</sup> J. Saren,<sup>4</sup> C. Scholey,<sup>4</sup> J. Sorri,<sup>4</sup> S. Stolze,<sup>4</sup> J. Uusitalo,<sup>4</sup> and M. Doncel<sup>6</sup>

<sup>1</sup>*School of Physics & Astronomy, The University of Manchester, Oxford Road, Manchester M13 9PL, United Kingdom*

<sup>2</sup>*Centro de Física das Interações Fundamentais/CeFEMA, Departamento de Física, Instituto Superior Tecnico, Avenida Rovisco Pais, P1049-001 Lisbon, Portugal*

<sup>3</sup>*Dipartimento di Fisica e Astronomia "G. Galilei", Istituto Nazionale di Fisica Nucleare, Via Marzolo 8, I-35131, Padova, Italy*

<sup>4</sup>*Department of Physics, University of Jyväskylä, Jyväskylä FIN-40014, Finland*

<sup>5</sup>*CSNSM, CNRS/IN2P3 and Université Paris Sud, F-91405 Orsay, France*

<sup>6</sup>*Department of Physics, Royal Institute of Technology, Stockholm, SE-10691, Sweden*

(Received 14 November 2014; revised manuscript received 22 January 2015; published 24 April 2015)

Gamma rays from excited states feeding a proton-emitting isomeric-state in  $^{151}\text{Lu}$  have been observed for the first time. Comparison with state-of-the-art nonadiabatic quasiparticle calculations indicates an oblatelly deformed,  $3/2^+$  proton-emitting state with a quadrupole deformation of  $\beta_2 = -0.11$ . The calculations suggest an increase in quadrupole deformation, to  $\beta_2 = -0.18$ , with increasing spin which is understood in terms of the mixing of Nilsson states at the Fermi surface. It is also shown that the proton decay half-life is consistent with that from a  $3/2^+$  state with a quadrupole deformation of  $\beta_2 = -0.12$ .

DOI: [10.1103/PhysRevC.91.044322](https://doi.org/10.1103/PhysRevC.91.044322)

PACS number(s): 21.60.-n, 21.10.Gv, 23.20.Lv, 27.60.+j

### I. INTRODUCTION

The proton drip line defines one of the fundamental limits to nuclear stability. Nuclei lying beyond this locus are energetically unbound to the emission of a constituent proton from their ground state [1]. Nuclear structure information on proton emitting nuclei can be extracted from a comparison of the measured proton decay half-lives with those predicted by tunneling calculations. Proton decay rates for near-spherical nuclei in the region  $N = 50$ – $82$  have been shown to be well reproduced by simple Wentzel-Kramers-Brillouin (WKB) calculations using spectroscopic factors derived from a low-seniority spherical shell-model calculation [2]; however, more sophisticated models are required for deformed nuclei [3,4].

Ground-state proton emission was first observed in  $^{151}\text{Lu}$  [5], where a decay half-life of 85(10) ms was measured. In order to interpret this, WKB theoretical tunneling calculations were performed based upon a spherical nuclear potential [6]. The use of a spherical potential was, at that time, justified by the close proximity of  $^{151}\text{Lu}$  to the  $N = 82$  shell closure. These spherical calculations were indeed able to provide a satisfactory agreement with the experimental half-life based upon a proton with angular momentum  $l = 5$ , originating from the spherical  $h_{11/2}$  single-particle orbital which formed the ground state. Several years later, proton emission was also observed from a low-lying isomeric state in  $^{151}\text{Lu}$  with a half-life of 16  $\mu\text{s}$  [7]. In an analogous manner to the ground-state calculations, based upon a spherical potential, proton decay from the isomeric state was described as an  $l = 2$  decay from a spherical  $d_{3/2}$  single-particle state. In that work, however, it was acknowledged that larger than expected spectroscopic

factors were required in order to obtain agreement with the experimental emission rates. The discrepancy was explained as either due to possible shifts in the relative energies of the  $d_{3/2}$  and  $h_{11/2}$  states, or from the effects of core excitations from the coupling of the single-particle states to the  $2^+$  state of  $^{150}\text{Yb}$  [7]. To try to address this discrepancy, data collected from an experiment which measured the lifetime of the  $(15/2^-)$  state above the proton-emitting  $11/2^-$  ground state [8] has been re-analyzed in this work. Shorter proton-decay correlation times have been employed in a bid to observe the previously reported isomeric decay as well previously unobserved  $\gamma$  rays that feed the proton-emitting state.

### II. EXPERIMENTAL DETAILS

The experiment was performed at the Accelerator Laboratory of the University of Jyväskylä, Finland. A beam of  $^{58}\text{Ni}^{8+}$  ions at 290 MeV was accelerated onto a  $550 \mu\text{g cm}^{-2}$   $^{96}\text{Ru}$  target, mounted on an upstream-facing  $2 \text{ mg cm}^{-2}$  Au backing. Prompt  $\gamma$ -ray transitions were measured in the Jurogam-II spectrometer [9] positioned around the target. Recoiling fusion-evaporation residues were separated in flight from scattered beam by RITU, the gas-filled separator [10,11]. RITU operated with a helium gas pressure of 0.6 mbar and was partitioned from the vacuum of the beam line by a differential pumping system. Recoils were transported to the GREAT focal-plane spectrometer [12] where they were implanted into a pair of double-sided silicon strip detectors (DSSDs). A multiwire proportional counter (MWPC) upstream of the DSSDs was used to help discriminate between scattered beam, evaporation residues and decays. The high granularity of the DSSDs allowed fusion-evaporation products to be identified as  $^{151}\text{Lu}$  through the use of the recoil-decay tagging (RDT) technique [13,14]. The Differential Plunger for Unbound Nuclear States (DPUNS) [15] was located at the

\*Present address: Department of Physics, Royal Institute of Technology, SE-10691 Stockholm, Sweden.

target position to facilitate the collection of recoil distance Doppler shift (RDDS) data were not used in the present work. Data were time stamped by a 100 MHz clock from the Total Data Readout (TDR) acquisition system [16] and sorted into one-dimensional histograms and two-dimensional matrices using the GRAIN data analysis package [17].

### III. RESULTS

Figure 1 shows DSSD spectra for decays which had no MWPC signal following a recoil implantation in the same DSSD pixel. Figure 1(a) has a recoil-decay time condition of 400 ms, which is approximately  $5 \times t_{1/2}$  for the ground-state proton decay in  $^{151}\text{Lu}$  as reported in Ref. [5]. Although the spectrum is dominated above 3.5 MeV by  $\alpha$ -decay lines, a peak is visible at 1232(4) keV which is consistent with the ground-state proton decay energy of  $^{151}\text{Lu}$ , 1233(3) keV [18].

Figure 1(b) has a recoil-decay time condition of 80  $\mu\text{s}$ , approximately  $5 \times t_{1/2}$  of the isomeric proton decay in  $^{151}\text{Lu}$  as reported in Ref. [7]. This time condition greatly suppresses the longer lived alpha decay lines and shows a proton decay peak at 1285(4) keV. This mean energy is slightly lower but consistent with the current literature value of 1310(10) keV [18]. In this work, the energy calibration was performed with a quadratic least-squares fit to the  $^{151}\text{Lu}$  ground-state proton decay and the known  $^{151}\text{Dy}$ ,  $^{150}\text{Dy}$ ,  $^{151}\text{Ho}$ ,  $^{151m}\text{Ho}$ , and  $^{152}\text{Er}$   $\alpha$  decay lines shown in Fig. 1(a). Details of the energy calibration process used in the previously published measurement are not extensive and only mention the ground-state proton-decay energy being used [7]. In the present work the measured isomeric proton-decay energy yields an energy difference of 53(6) keV between the isomeric and ground states. The competing 53 keV  $\gamma$ -decay branch was not observed by the Jurogam-II array, possibly due to the relatively low efficiency at this energy.

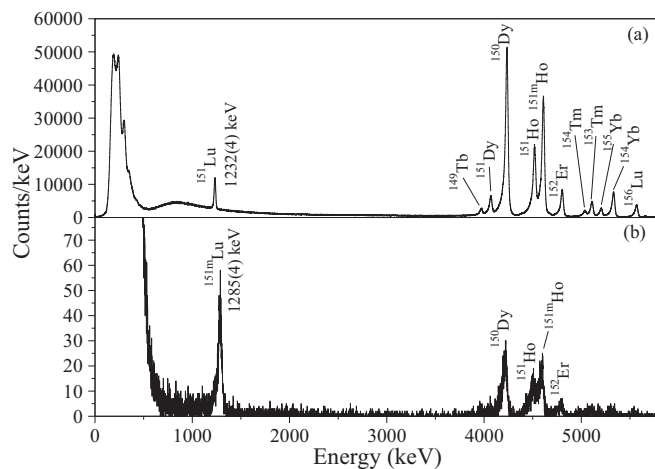


FIG. 1. Double-sided Si strip detector spectra showing charged particle decays following a recoil implantation. (a) Decays recorded within 400 ms of a recoil implantation. A background spectrum of decays recorded between 1 and 1.4 s has been subtracted. (b) Decays recorded within 80  $\mu\text{s}$  of a recoil implantation. A background spectrum of decays recorded between 310 and 390  $\mu\text{s}$  has been subtracted.

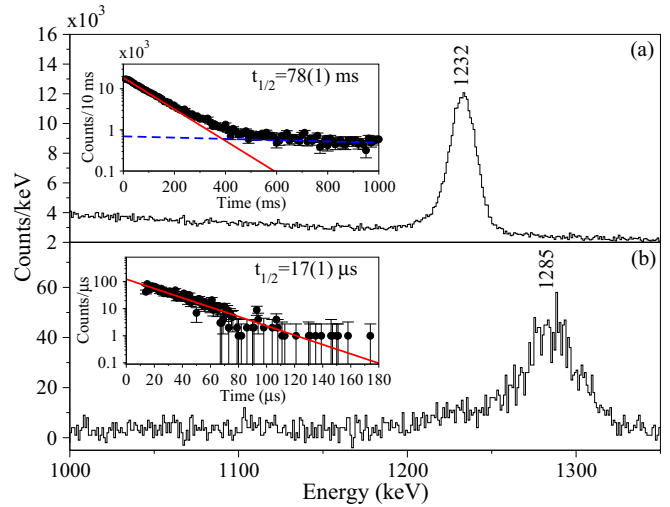


FIG. 2. (Color online) Low energy portions of the time gated spectra shown in Fig. 1. The insets show the associated recoil-proton time distributions along with the results of exponential fits. The energies and half-lives for the 1232(4) keV decays in (a) and the 1285(4) keV decays in (b) are consistent with the current literature values for the ground-state and isomeric proton decays, respectively, from  $^{151}\text{Lu}$  [18].

Figure 2 shows low-energy portions of the spectra shown in Fig. 1 along with background subtracted recoil-proton time distributions (insets). For the ground-state decay a two-exponential fit is performed to account for random correlations arising from the relatively high recoil implantation rate compared to the decay rate [19]. Least-squares fits to the decay curves reveal half-lives of 78(1) ms and 17(1)  $\mu\text{s}$  for the 1232(4) and 1285(4) keV proton decays, respectively, consistent with the current literature values of 81(2) ms and 16(1)  $\mu\text{s}$  [18]. Gating on the proton decay peaks shown in Figs. 1 and 2 allows any correlated prompt  $\gamma$  rays, recorded in the Jurogam II detectors, to be investigated. Figure 3(a) shows prompt  $\gamma$  rays that correlate with  $^{151}\text{Lu}$  ground-state proton-decays occurring within 400 ms after a recoil implantation. All of the  $\gamma$  rays observed in this spectrum are reported in our previous work [8] with the exception of a 625 keV decay. Using a proton gated  $\gamma$ - $\gamma$  matrix and multiple gating conditions the location of the 625 keV decay has now been established. Figure 4 shows double-gated  $\gamma$ -ray spectra produced from a ground-state proton decay gated prompt  $\gamma$ - $\gamma$  matrix. Figure 4(a) contains  $\gamma$  rays that correlate with the 861 or 611 keV decays depopulating the  $(19/2^-)$  and  $(15/2^-)$  states, respectively. The 625 keV decay clearly correlates with both of these transitions. Figure 4(b) shows  $\gamma$  rays that correlate with the 322 or 951 keV decays that depopulate the two states,  $(27/2^-)$  and  $(23/2^-)$ , respectively, that feed into the  $(19/2^-)$  state. It is clear from the spectrum in Fig. 4(b) that the 625 keV decay does not correlate with either the 322 or the 951 keV transitions indicating that the 625 keV belongs to a different structure that feeds into the  $(19/2^-)$  state. Figure 4(c) shows  $\gamma$  rays that correlate with 301, 402, or 684 keV decays that depopulate the  $(21/2^+)$ ,  $(21/2^-)$ , and  $(29/2^+)$  states, respectively. The level scheme published in

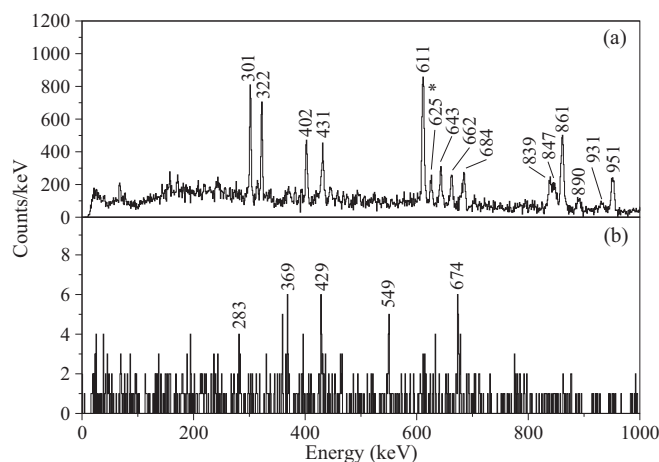


FIG. 3. Background subtracted, prompt  $\gamma$  rays recorded by the Jurogam II detectors that correlate with proton decays recorded in the focal plane DSSD detectors. (a)  $\gamma$  rays that correlate within 400 ms of a ground-state proton decay. The starred line at 625 keV is a previously unobserved decay. (b)  $\gamma$  rays that correlate within 80  $\mu$ s of an isomeric-state proton decay.

Ref. [8] has the 684 keV decay depopulating a  $(25/2^+)$  state and thus the order of the 684 and 849 keV decays reversed compared to the scheme of this work; see Fig. 5. Based on the measured intensities of the 625, 684, and 847 keV  $\gamma$  rays in this work, it is proposed that the 625 keV  $\gamma$  ray resides above the 684 and 847 keV decays and depopulates a  $(33/2^+)$  state. A parallel analysis of data collected in a separate, unpublished, experiment on  $^{151}\text{Lu}$  agrees with this placement [20].

Figure 3(b) is a spectrum of prompt  $\gamma$  rays that correlate with an isomeric proton-decay occurring within 80  $\mu$ s after a recoil implantation. Five  $\gamma$  rays with energies 283, 369, 429, 549, and 674 keV are observed. It is important to

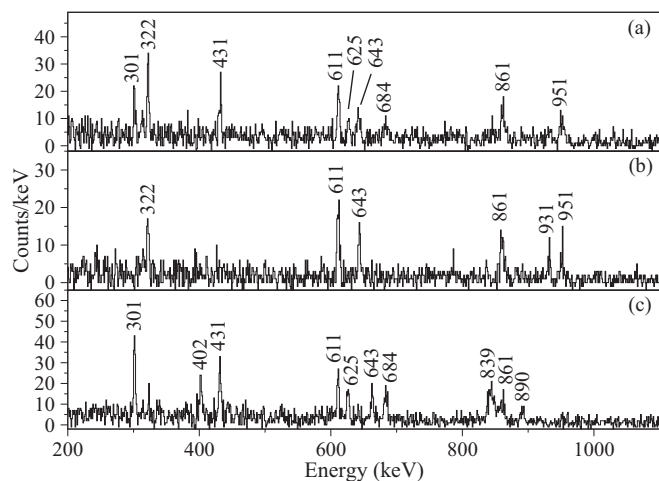


FIG. 4. Background subtracted prompt Jurogam II  $\gamma$ -ray spectra produced from gates on a recoil-decay (ground-state proton) tagged  $\gamma$ - $\gamma$  matrix. (a) 611 and 861 keV gated sum spectrum. (b) 322 and 951 keV gated sum spectrum. (c) 301, 402, and 684 keV gated sum spectrum.

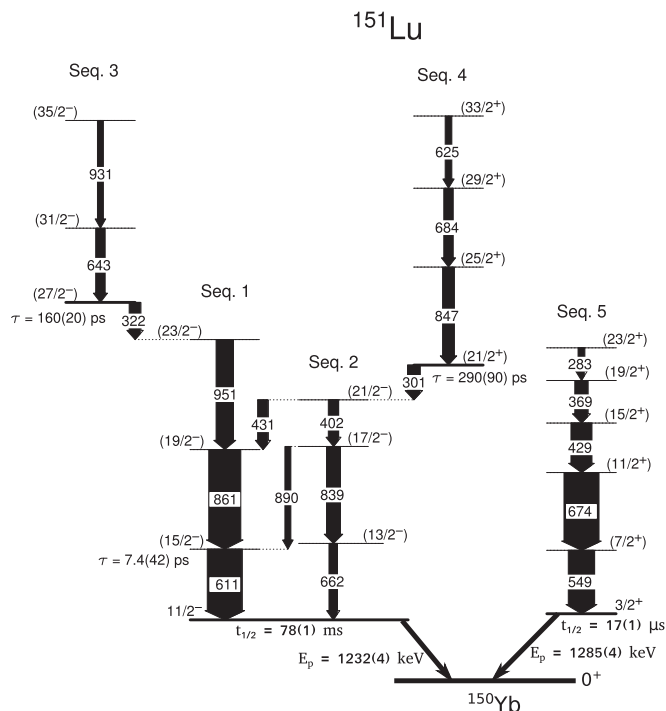


FIG. 5. Partial decay scheme for  $^{151}\text{Lu}$  showing the newly observed decays built upon the  $3/2^+$  isomeric proton-emitting state (decay sequence 5) in  $^{151}\text{Lu}$ . The previously observed (sequences 1–4) states [8] above the  $11/2^-$  ground state are also shown with the addition of the 625 keV decay whose location was verified in this work. The proton-decay half-lives quoted are those measured in this work. The ordering of the 549 and 674 keV transitions is based on the results of calculations discussed in Sec. IV A. Bracketed spins and parities are tentative.

note that none of these transitions appear in the ground-state proton-decay correlated  $\gamma$ -ray spectrum shown in Fig. 3(a). A tentative ordering for these  $\gamma$  rays was established based on efficiency-corrected measured intensities. Figure 5 shows a partial decay scheme produced from the proton-gated spectra of Fig. 3 with tentative spin-parity assignments in brackets. A 130 keV  $\gamma$  ray corresponding to the  $(21/2^+) \rightarrow (19/2^+)$  transition is not observed. The measured intensities for the 847 and 301 keV  $\gamma$  rays alone can account for the total flux through the isomeric  $(21/2^+)$  state; similarly for the 283 and 369 keV  $\gamma$  rays, within the large uncertainties, populating and depopulating the  $(19/2^+)$  state, respectively. The absence of this 130 keV linking transition could indicate a more significant structural change between sequences 4 and 5 than between sequences 4 and 2.

The low statistical nature of the collected data does not allow a detailed understanding of the  $(21/2^+)$  and  $(27/2^-)$  isomers shown in Fig. 5. The level scheme of Ref. [8] reports the  $(21/2^+)$  isomeric decay as an  $M1$  feeding a  $(19/2^+)$  state. The  $(19/2^+)$  state then decays via competing  $E1$  and  $M1$  transitions. In the present work the  $(21/2^+)$  isomer is shown to depopulate via a hindered  $E1$  decay which feeds into a  $(21/2^-)$  state. The  $(21/2^-)$  state would then decay via competing  $M1$  and  $E2$  transitions. A hindered  $E1$  decay could explain

TABLE I. Energies and efficiency-corrected relative intensities for the transitions shown in Fig. 5. The upper portion is for the transitions in sequences 1 to 4 that feed into the  $11/2^-$  state and the lower portion for sequence 5 that feeds into the  $3/2^+$  state.

$E_\gamma$ (keV)	$J_i^\pi \rightarrow J_f^\pi$	$I_\gamma$ (%)
301.3(3)	$(21/2^+) \rightarrow (21/2^-)$	36(3)
321.7(3)	$(25/2^-) \rightarrow (23/2^-)$	32(3)
402.0(50)	$(21/2^-) \rightarrow (17/2^-)$	29(3)
430.8(5)	$(21/2^-) \rightarrow (19/2^-)$	29(3)
611.0(3)	$(15/2^-) \rightarrow (11/2^-)$	100(6)
625.4(7)	$(33/2^+) \rightarrow (29/2^+)$	19(3)
642.7(6)	$(29/2^-) \rightarrow (25/2^-)$	27(3)
662.0(7)	$(13/2^-) \rightarrow (11/2^-)$	24(3)
683.9(6)	$(29/2^+) \rightarrow (25/2^+)$	27(3)
838.6(8)	$(17/2^-) \rightarrow (13/2^-)$	40(4)
846.9(9)	$(25/2^+) \rightarrow (21/2^+)$	34(4)
860.6(5)	$(19/2^-) \rightarrow (15/2^-)$	92(7)
889.6(12)	$(17/2^-) \rightarrow (15/2^-)$	17(3)
931.2(12)	$(33/2^-) \rightarrow (29/2^-)$	17(4)
950.6(7)	$(23/2^-) \rightarrow (19/2^-)$	50(7)
283.0(44)	$(23/2^+) \rightarrow (19/2^+)$	18(10)
368.6(34)	$(19/2^+) \rightarrow (15/2^+)$	37(16)
428.8(28)	$(15/2^+) \rightarrow (11/2^+)$	59(22)
549.4(27)	$(7/2^+) \rightarrow (3/2^+)$	75(27)
673.7(25)	$(11/2^+) \rightarrow (7/2^+)$	100(34)

the  $(21/2^+)$  state isomerism. Table I lists the energies and efficiency-corrected relative intensities of the  $\gamma$  rays measured in this work with the upper portion for sequences 1 to 4 and the lower portion for sequence 5 as shown in Fig. 5. The ordering of the 549 and 674 keV transitions in sequence 5, whose intensities are consistent, is based on the result of calculations discussed in Sec. IV A.

#### IV. DISCUSSION

Since the discovery of proton emission from  $^{151}\text{Lu}$ , a number of other proton emitters have been observed in the  $A \approx 150$  region [21–23]. The lightest proton-emitting Lu isotope observed to date is  $^{150}\text{Lu}$  where decays from the ground-state were measured with an energy of 1261(4) keV and a half-life of 35(10) ms [23]. In that work, ground-state proton decays from  $^{151}\text{Lu}$  were also observed but no evidence was presented for an isomeric proton-decaying state, presumably due to low statistics. The only other nucleus in the  $A \approx 150$  region for which  $\gamma$  emission from an excited state above an isomeric proton-emitting state has been observed is  $^{147}\text{Tm}$  [22]. A 587 keV  $\gamma$ -ray transition from a proposed  $(5/2^+)$  state was placed above the proton-emitting  $3/2^+$  state in  $^{147}\text{Tm}$ . Due to the low intensity, the placement was reported to be uncertain and the tentative  $(5/2^+)$  assignment was based on a comparison with the systematics in the lighter  $N = 78$  isotones. In order to shed light on the configurations of the states above the isomeric proton-emitting state in  $^{151}\text{Lu}$ , state-of-the-art nonadiabatic calculations have been performed in the present work.

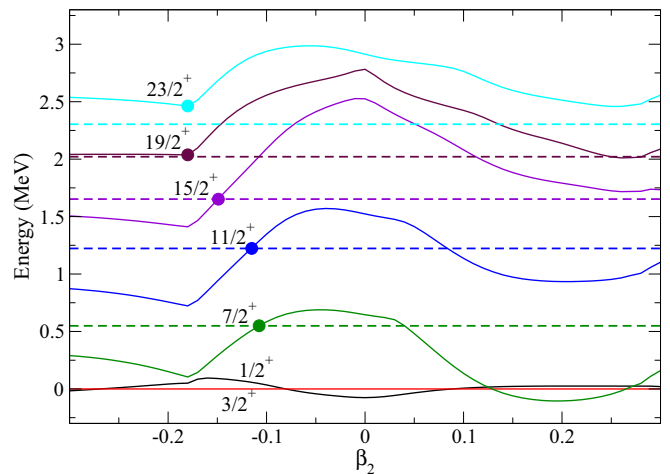


FIG. 6. (Color online) Comparison between the results from the nonadiabatic quasiparticle calculations and experiment. Solid lines are the calculated energies as a function of quadrupole deformation and the dashed lines are the corresponding experimental energies. The circles represent the closest match between theory and experiment.

#### A. Nonadiabatic quasiparticle model

Theoretical calculations have been performed using a new nonadiabatic quasiparticle model [24], modified to take into account the experimental spectrum of the core. The framework uses a quasiparticle plus a deformed core approach with the mean field represented by a Woods-Saxon potential with a deformed spin-orbit interaction. These calculations are an extension of those performed for the work presented in Ref. [8].

Figure 6 shows the calculated excited-state energies (solid lines) as a function of quadrupole deformation. The experimentally determined energies are denoted by dashed lines. The filled circles displayed in Fig. 6 are placed at the best agreement between the experimental and theoretical energies. The calculated energies have been normalized to that of the  $3/2^+$  state. For small values of quadrupole deformation  $|\beta_2| \lesssim 0.1$  the  $1/2^+$  state is lowest in energy. For larger values of deformation the  $3/2^+$  is lowest in energy until a very large oblate deformation of  $\beta_2 \approx -0.25$  is reached, after which the  $1/2^+$  state once again is lower in energy.

Although the relative intensities of the two lowest spin transitions in decay sequence 5 have been measured as 100(34) and 75(27), within experimental uncertainties the ordering could be reversed. A  $(7/2^+)$  state energy of 674 keV would correspond to a quadrupole deformation of  $\beta_2 = -0.07$  with the  $1/2^+$  state becoming the proton-emitting state at this deformation. A  $1/2^+$  proton-emitting state would also result if prolate deformation for the sequence was assumed; however, the ordering would not be consistent with the regular structure associated with a prolate-deformed rotor. Figure 7 shows the calculated proton-decay half-life, as a function of quadrupole deformation, for decays originating from  $1/2^+$  and  $3/2^+$  states in  $^{151}\text{Lu}$ . A weighted mean, 16.5(7)  $\mu\text{s}$ , of the experimental half-life determined in this work and that previously measured by Bingham *et al.* [7] is shown by the horizontal line whose thickness is proportional to the associated uncertainty. It is evident from Fig. 7 that the experimental decay half-life is

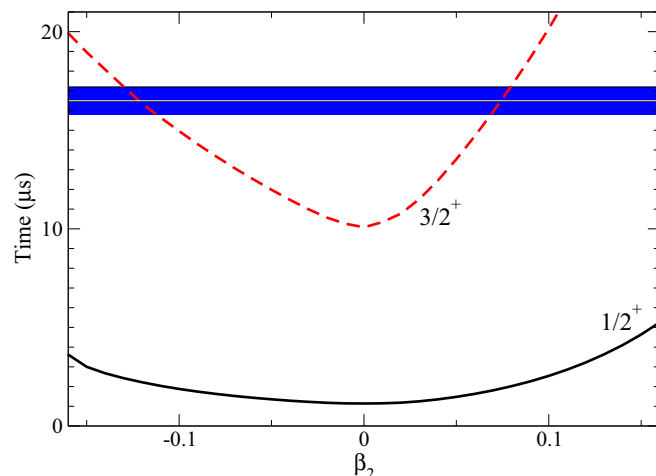


FIG. 7. (Color online) A plot showing the proton decay half-life as a function deformation for the  $1/2^+$  (solid line) and  $3/2^+$  (dashed line) states. A weighted mean half-life using the current literature value and that measured in this work is shown (thick horizontal line) where the thickness of the line represents the measurement uncertainty.

only consistent with proton emission from a  $3/2^+$  state. Based on this evidence, the level ordering shown in Fig. 5 is adopted with the 674 keV  $\gamma$  ray depopulating the ( $11/2^+$ ) state. This  $3/2^+$  assignment for the isomeric proton-emitting state is in agreement with the WKB analysis of Bingham *et al.* [7]. In that work, it was concluded that, for a spherical potential, larger than expected spectroscopic factors were required to explain the measured proton-emission rate and that the discrepancy between the measured and calculated rates could be explained by a possible shift in the relative energies of the  $d_{3/2}$  and  $h_{11/2}$  states [7]. The difference in energy for the measured proton decay from this work to that from Ref. [7] would have the effect of increasing the half-life by a factor of 1.76. Scaling the WKB calculated half-life [7] by 1.76 results in a half-life of 10  $\mu$ s in agreement with the present nonadiabatic model for zero deformation. This value is still some way off the adopted half-life of 16.5(7)  $\mu$ s. This means the newly measured proton-decay energy from the isomeric state cannot explain the discrepancy in the required spectroscopic factors alluded to by Bingham *et al.* [7]. As shown in Fig. 7, however, agreement between calculated and measured half-life can be obtained if deformation is invoked.

Figure 8 shows a comparison between the experimentally observed and the theoretically calculated excited states above the  $3/2^+$  proton-emitting isomer. The theoretical state energies have been extracted from Fig. 6 for the  $\beta_2$  values shown (filled circles). The predicted quadrupole deformation of the  $3/2^+$  state, based on the observed trend in Fig. 6 and the calculated  $\beta_2$  for the ( $7/2^+$ ) state, is also shown. The low-spin states are easily formed in the model by coupling the odd  $s_{1/2}$  or  $d_{3/2}$  proton to a  $0^+$  or  $2^+$  core. However, to generate higher angular momentum states, with this proton configuration, a higher angular momentum from the core would be required which becomes energetically unfavorable. At low oblate deformation, the Nilsson states  $1/2[411]$  and  $3/2[402]$  are

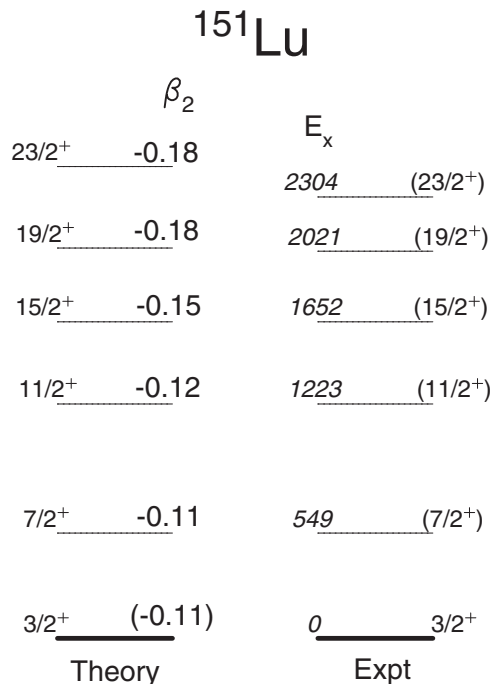


FIG. 8. Partial level schemes showing the best agreement, in energy, between the experimentally determined states above the isomeric proton-emitting  $3/2^+$  state and those determined from the nonadiabatic quasiparticle calculations. The calculated quadrupole deformation parameters,  $\beta_2$ , are also shown.

close to the Fermi surface and are quite pure mixtures of  $d_{3/2}$  and  $s_{1/2}$  configurations. As deformation increases other states, for example the  $1/2[420]$ ,  $3/2[411]$  states from the  $d_{5/2}$  shell and the  $1/2[431]$ ,  $3/2[422]$  states from the  $g_{7/2}$  shell, approach the Fermi surface and interact. At a deformation of around  $\beta_2 \approx -0.15$  the wave functions of the  $1/2[411]$  and  $3/2[402]$  states are no longer predominantly  $d_{3/2}$  and  $s_{1/2}$  in character. Thus, with a slight increase in deformation the angular momentum of the odd proton increases. This is an energetically more favorable method for generating the higher spin states than raising the angular momentum of the  $^{150}\text{Yb}$  core. The comparison between theory and experiment in Fig. 6 suggests an increase in quadrupole deformation above the ( $11/2^+$ ) state.

The extrapolated  $\beta_2 = -0.11$  for the  $3/2^+$  state from Fig. 6 is very close to the value that reproduces the experimental half-life for proton emission,  $\beta_2 = -0.12$  (see Fig. 7). Oblate deformation was also deduced for the  $11/2^-$  proton-emitting ground state [8]. The theoretical and experimental data shown in Figs. 6 and 7 strongly suggest an oblatel deformed  $3/2^+$  state for the isomeric proton-emitting state in  $^{151}\text{Lu}$ .

## V. SUMMARY

Gamma-ray transitions between excited states residing above an isomeric proton-emitting state have been observed for the first time in the drip-line nucleus  $^{151}\text{Lu}$ . A decay scheme has been proposed based on the measured transition intensities and theoretical calculations. Nonadiabatic quasiparticle

calculations have been performed to determine the isomeric state configuration and deformation. Best agreement between the experimental and theoretical decay-schemes suggests an oblate deformation for the proton-emitting  $3/2^+$  state with a quadrupole deformation of  $\beta_2 = -0.11$ . A comparison between theoretical and experimental data also suggests an increase in quadrupole deformation with increasing spin. This can be explained by the increased influence of high angular momentum configurations in the Nilsson states at the Fermi surface.

The calculations showed that the experimentally determined half-life is consistent with emission from a  $3/2^+$  state with a quadrupole deformation of  $\beta_2 \approx -0.12$ . The disagreement between the experimental proton-decay half-life and that calculated within the spherical WKB formalism by Bingham *et al.* [7] is not resolved using the lower  $3/2^+$  state energy measured in this work. Agreement between

the measured and calculated proton-decay half-lives is only reached with the inclusion of deformation.

#### ACKNOWLEDGMENTS

This work has been supported by the EU 7th Framework Programme, “Integrating Activities – Transnational Access,” Project No. 262010 (ENSAR), and by the Academy of Finland under the Finnish Centre of Excellence Programme (Nuclear and Accelerator Based Physics Programme at JYFL). The authors acknowledge the support of GAMMAPOOL for the loan of the Jurogam detectors. Theoretical work by L.S.F. and E.M. was supported by the Fundação para a Ciência e a Tecnologia (Portugal), Project No. CERN/FP/123606/2011. T.G. acknowledges the support of the Academy of Finland under Contract No. 131665. The authors also wish to thank Prof. R. Wadsworth for the loan of the  $^{96}\text{Ru}$  target.

- 
- [1] P. J. Woods and C. N. Davids, *Annu. Rev. Nucl. Part. Sci.* **47**, 541 (1997).
- [2] C. N. Davids, P. J. Woods, J. C. Batchelder, C. R. Bingham, D. J. Blumenthal, L. T. Brown, B. C. Busse, L. F. Conticchio, T. Davinson, S. J. Freeman *et al.*, *Phys. Rev. C* **55**, 2255 (1997).
- [3] E. Maglione, L. S. Ferreira, and R. J. Liotta, *Phys. Rev. Lett.* **81**, 538 (1998).
- [4] L. S. Ferreira and E. Maglione, *Phys. Rev. C* **61**, 021304 (2000).
- [5] S. Hofmann, W. Reisdorf, G. Münzenberg, F. P. Heßberger, J. R. H. Schneider, and P. Armbruster, *Z. Phys. A* **305**, 111 (1982).
- [6] S. Hofmann, *Nuclear Decay Models* (IOP, Bristol, 1996).
- [7] C. R. Bingham, J. C. Batchelder, K. Rykaczewski, K. S. Toth, C.-H. Yu, T. N. Ginter, C. J. Gross, R. Grzywacz, M. Karny, S. H. Kim *et al.*, *Phys. Rev. C* **59**, 2984R (1999).
- [8] M. G. Procter, D. M. Cullen, M. J. Taylor, G. A. Alharshan, L. S. Ferreira, E. Maglione, K. Auranen, T. Grahn, P. T. Greenlees, U. Jakobsson *et al.*, *Phys. Lett. B* **725**, 79 (2013).
- [9] P. J. Nolan, F. A. Beck, and D. B. Fossan, *Annu. Rev. Nucl. Part. Sci.* **44**, 561 (1994).
- [10] M. Leino, J. Äystö, T. Enqvist, P. Heikkinen, A. Jokinen, M. Nurmia, A. Ostrowski, W. H. Trzaska, J. Uusitalo, K. Eskola *et al.*, *Nucl. Instrum. Methods Phys. Res., Sect. B* **99**, 653 (1995).
- [11] J. Sarén, J. Uusitalo, M. Leino, and J. Sorri, *Nucl. Instrum. Methods Phys. Res., Sect. A* **654**, 508 (2011).
- [12] R. D. Page, A. N. Andreyev, D. E. Appelbe, P. A. Butler, S. J. Freeman, P. T. Greenlees, R.-D. Herzberg, D. G. Jenkins, G. D. Jones, P. Jones *et al.*, *Nucl. Instrum. Methods Phys. Res., Sect. B* **204**, 634 (2003).
- [13] K.-H. Schmidt, R. S. Simon, J.-G. Keller, F. P. Hessberger, G. Münzenberg, B. Quint, H.-G. Clerc, W. Schwab, U. Gollerthan, and C.-C. Sahn, *Phys. Lett. B* **168**, 39 (1986).
- [14] E. S. Paul, P. J. Woods, T. Davinson, R. D. Page, P. J. Sellin, C. W. Beausang, R. M. Clark, R. A. Cunningham, S. A. Forbes, D. B. Fossan *et al.*, *Phys. Rev. C* **51**, 78 (1995).
- [15] M. J. Taylor, D. M. Cullen, A. J. Smith, A. McFarlane, V. Twist, G. A. Alharshan, M. G. Procter, T. Braunroth, A. Dewald, E. Ellinger *et al.*, *Nucl. Instrum. Methods Phys. Res., Sect. A* **707**, 143 (2013).
- [16] I. Lazarus, E. E. Appelbe, P. A. Butler, P. J. Coleman-Smith, J. R. Cresswell, S. J. Freeman, R. D. Herzberg, I. Hibbert, D. T. Joss, S. C. Letts *et al.*, *IEEE Trans. Nucl. Sci.* **48**, 567 (2001).
- [17] P. Rakhila, *Nucl. Instrum. Methods Phys. Res., Sect. A* **595**, 637 (2008).
- [18] B. Singh, *Nucl. Data Sheets* **110**, 1 (2009).
- [19] M. E. Leino, S. Yashita, and A. Ghiorso, *Phys. Rev. C* **24**, 2370 (1981).
- [20] F. Wang, B. Sun, Z. Liu, C. Scholey, S. Ashley, L. Bianco, D. Cullen, I. Cullen, I. Darby, and S. Eeckhaudt (unpublished).
- [21] R. J. Irvine, C. N. Davids, P. J. Woods, D. J. Blumenthal, L. T. Brown, L. F. Conticchio, T. Davinson, D. J. Henderson, J. A. MacKenzie, H. T. Penttilä *et al.*, *Phys. Rev. C* **55**, R1621 (1997).
- [22] D. Seweryniak, C. N. Davids, W. B. Walters, P. J. Woods, I. Ahmad, H. Amro, D. J. Blumenthal, L. T. Brown, M. P. Carpenter, T. Davinson *et al.*, *Phys. Rev. C* **55**, R2137 (1997).
- [23] P. J. Sellin, P. J. Woods, T. Davinson, N. J. Davis, K. Livingston, R. D. Page, A. C. Shotton, S. Hofmann, and A. N. James, *Phys. Rev. C* **47**, 1933 (1993).
- [24] G. Fiorin, E. Maglione, and L. S. Ferreira, *Phys. Rev. C* **67**, 054302 (2003).